Influence of Gap Extrema on the Tunneling Conductance Near an Impurity in an Anisotropic Superconductor

J. M. Byers,[1] M. E. Flatté,[2,*] and D. J. Scalapino[1]
[1]*Department of Physics, University of California, Santa Barbara, California 93106-9530*
[2]*Institute for Theoretical Physics, University of California, Santa Barbara, California 93106-4030*
(Received 22 June 1993)

We examine the effect of an impurity on the nearby tunneling conductance in an anisotropically gapped superconductor. The variation of the conductance has pronounced spatial dependence which depends strongly on the Fermi surface location of gap extrema. In particular, different gap symmetries produce profoundly different spatial features in the conductance. These effects may be detectable with a scanning-tunneling-microscope study of the surface of a high-temperature superconductor.

PACS numbers: 74.50.+r, 74.80.–g

Any well-developed theory of high-temperature superconductivity must predict the symmetry of the energy gap. Some proposals, including the strongly coupled phonon-mediated pairing which causes superconductivity in ordinary metals [1], yield isotropic or nearly isotropic gaps. The dominant characteristic of the pairing interaction in this model is retardation. In the low-temperature superconductors this is reflected in the frequency dependence of the superconducting gap and clearly shows that phonons mediate the pairing.

For a nearly half-filled Hubbard model, approximations involving the exchange of para-antiferromagnetic spin fluctuations give rise to an effective electron-electron interaction which has a characteristic momentum dependence, peaking near the antiferromagnetic wave vector [2, 3]. A similar momentum dependence has been found in Monte Carlo simulations [4]. Such an interaction favors $d_{x^2-y^2}$ pairing and gives rise to a momentum-dependent gap which has four nodes.

Gap-measurement techniques that were introduced and developed for use on electron-phonon superconductors measure accurately the frequency structure of the gap. Among these are the voltage dependence of the tunneling $I(V)$ characteristic into the homogeneous superconductor [5] and the frequency dependence of electromagnetic absorption [6]. If, however, the gap has strong momentum dependence these measurements depend on some momentum-averaged value of the gap. Most of these probes [7, 8] now indicate pronounced gap anisotropy or gapless superconductivity in the high-temperature superconductors.

In the cuprate-oxide superconductors it would be useful to have experimental information on the momentum dependence of the gap. Certain techniques exist which are designed to detect gap nodes on the Fermi surface. These include measurements of the low-temperature dependence of thermodynamic and transport properties, such as the specific heat [9] and the magnetic penetration depth [10]. Here power-law dependencies on temperature typically imply nodes, in contrast to the exponential behavior associated with a fully gapped Fermi surface. Measurements of these quantities proved extremely illuminating in studies of heavy-fermion materials [11]. Recent results [10] on $YBa_2Cu_3O_7$ indicate a low-temperature penetration depth proportional to T, suggesting the existence of nodes.

At this time, however, only a few experiments exist that directly measure the gap as a function of momentum on the Fermi surface. Angle-resolved photoemission (ARPES) on $Bi_2Sr_2CaCu_2O_8$ measures the magnitude of the gap [12] with an angular resolution of about 6° and an energy resolution of about 10 meV. A gap has been detected with ARPES only in $Bi_2Sr_2CaCu_2O_8$. Measurements of $YBa_2Cu_3O_7$ – Pb SQUIDs may eventually determine the symmetry of the superconducting gap [13], but do not provide detailed information on the momentum dependence of the gap. In theory, measurements of linewidth changes of phonons with finite momentum have excellent angular and energy resolution [14], and can measure the relative phase of the gap [15]. Such measurements have yet to be done.

Here we propose that a scanning-tunneling-microscope (STM) study of the spatial variation of the tunneling conductance [16] around an impurity can be used to probe the momentum dependence of the superconducting gap $\Delta_{\mathbf{k}}$. We will discuss in this Letter those features of the gap which produce the most profound changes in the local tunneling conductance: gap minima and maxima. A gap minimum or maximum on the Fermi surface produces strikingly large conductance variations along the spatial directions away from the impurity which are perpendicular to the Fermi surface tangent at the gap extremum. We numerically calculate the spatial structure for superconductors with (a) an isotropic gap, (b) a $d_{x^2-y^2}$ gap, and (c) an anisotropic but nodeless gap. The results are explained by analytic forms in various limits. The energies of gap maxima and minima should be discernible with a resolution better than 1 meV.

The feasibility of observing the local tunneling density of states with atomic resolution has been established by STM tunneling conductance measurements near impurities and step edges on the surface of Cu(111) [17].

In addition, tunneling conductances have been obtained with near-atomic resolution on the surface of the high-temperature superconductor $Bi_2Sr_2CaCu_2O_8$ [18].

We assume the impurity has three possible effects on the local environment in a superconductor: an impurity potential $\delta\epsilon$, a change in the superconducting gap $\delta\Delta_{\mathbf{k}}$ (which depends on the momentum $\mathbf{k}$), and a change in the local mass δm of the carriers. In our model each of these is a delta-function perturbation at an impurity site $\mathbf{0}$, perturbing the homogeneous Hamiltonian of the bulk superconductor. An impurity would actually have a finite-range effect on $\delta\epsilon$, $\delta\Delta_{\mathbf{k}}$, and δm, which could be as large as a superconducting coherence length. Here we will be concerned with conductance changes which persist at greater distances.

Each of the perturbations contributes to the others; for example, introducing an impurity potential will have an effect of the same order on the gap magnitude. This in turn affects the conductance. The precise relationship between the parameters depends upon details of the microscopic mechanism. We will use $\delta\epsilon$ and $\delta\Delta_{\mathbf{k}}$ as phenomenological parameters in our model, and assume that they satisfy the self-consistent equations for the superconductor. The effect of a δm can be absorbed into $\delta\epsilon$. We thus avoid the difficulty which results from attempting to start from "bare" impurity parameters.

The effect of the impurity perturbations on the conductance under the STM tip can be calculated from the Green's functions of the homogeneous superconductor. These are written compactly in the Nambu formalism [19]

$$\mathbf{G_0}(\mathbf{x},\mathbf{x}',\omega) = \begin{pmatrix} G_0(\mathbf{x},\mathbf{x}',\omega) & F_0(\mathbf{x},\mathbf{x}',\omega) \\ F_0(\mathbf{x},\mathbf{x}',\omega) & -G_0(\mathbf{x},\mathbf{x}',-\omega) \end{pmatrix}, \tag{1}$$

where

$$\begin{bmatrix} G_0(\mathbf{x},\mathbf{x}',\omega) \\ F_0(\mathbf{x},\mathbf{x}',\omega) \end{bmatrix} = \frac{1}{\mathcal{V}} \sum_{\mathbf{k}} \frac{e^{i\mathbf{k}\cdot(\mathbf{x}-\mathbf{x}')}}{\omega^2 - \epsilon_{\mathbf{k}}^2 - \Delta_{\mathbf{k}}^2 + i\eta} \begin{bmatrix} \omega + \epsilon_{\mathbf{k}} \\ \Delta_{\mathbf{k}} \end{bmatrix}. \tag{2}$$

Here $\epsilon_{\mathbf{k}}$ is the single-particle energy in the normal material, $\Delta_{\mathbf{k}}$ is the superconducting gap, $\mathbf{x}$ and $\mathbf{x}'$ are positions, ω is a frequency, and $\mathcal{V}$ is the volume. The conductance at a position $\mathbf{r}$ and voltage V is the imaginary part of the upper-left entry in the Nambu matrix: $dI(\mathbf{r},V)/dV = -A\,\mathrm{Im}G(\mathbf{r},\mathbf{r},\omega = V)$. Here A consists of voltage and position-independent matrix elements and numerical factors.

We find that the effect of $\delta\Delta_{\mathbf{k}}$ on the tunneling conductance is qualitatively indistinguishable from that of $\delta\epsilon$. Therefore, for brevity, we will present here our results on the effect of $\delta\epsilon$ only. The Green's function with an impurity at $\mathbf{0}$ to linear order in $\delta\epsilon$ is

$$\mathbf{G}(\mathbf{r},\mathbf{r},\omega) = \mathbf{G_0}(\mathbf{r},\mathbf{r},\omega) + \mathbf{G_0}(\mathbf{r},\mathbf{0},\omega)\delta\epsilon\tau_3\mathbf{G_0}(\mathbf{0},\mathbf{r},\omega), \tag{3}$$

where τ_3 is a Pauli matrix. Since the Green's functions only depend on $|\mathbf{x}-\mathbf{x}'|$, the two position variables $\mathbf{x}$ and $\mathbf{x}'$ will be replaced by $|\mathbf{x}-\mathbf{x}'|$ below.

It is useful to express the conductance in terms of dimensionless quantities. We define Green's functions normalized by the density of states at the Fermi energy N^*, such as $g_0 = G_0/N^*$. Then, in terms of the normalized coupling $\delta\tilde{\epsilon} = \delta\epsilon N^*$, the conductance at $\mathbf{r}$ is

$$\frac{dI(\mathbf{r},V)}{dV} = -\mathrm{Im}g_0(\mathbf{0},V) - \delta\tilde{\epsilon}\,\mathrm{Im}\left\{g_0^2(\mathbf{r},V) - f_0^2(\mathbf{r},V)\right\}, \tag{4}$$

where $dI(\mathbf{r},V)/dV$ is normalized by the normal metal's conductance.

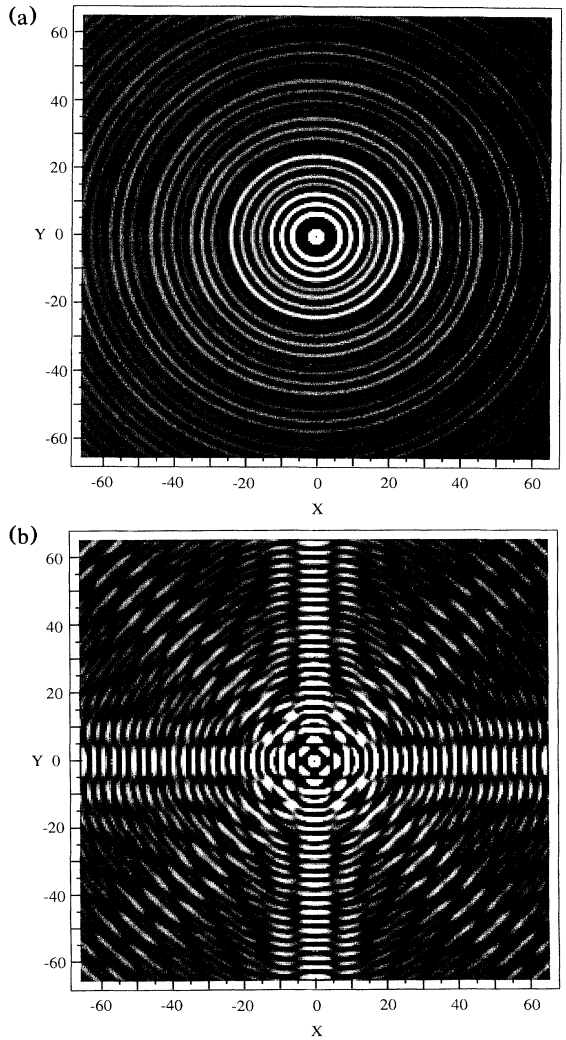

FIG. 1. Normalized conductance for a unit perturbation to the site energy $\delta\tilde{\epsilon}$. The length scale is set by k_F^{-1}. Here we have taken a coherence length equal to $10k_F^{-1}$. The voltage is $1.1\Delta_0$, where Δ_0 is the gap maximum. The range of the intensity is from -0.1 (black) to 0.1 (white). (a) Isotropic gap, $\Delta(\phi) = \Delta_0$; (b) $d_{x^2-y^2}$ gap, $\Delta(\phi) = \Delta_0 \cos 2\phi$.

We have plotted in Fig. 1 the normalized conductance (not including the bulk term) from Eq. (4) for $\delta\tilde{\epsilon} = 1$ for two gaps: (a) an isotropic gap, $\Delta(\phi) = \Delta_0$ and (b) a $d_{x^2-y^2}$ gap, $\Delta(\phi) = \Delta_0 \cos 2\phi$. The bias V is set to $1.1\Delta_0$. Strong angular dependence of the signal in Fig. 1(b) is apparent. We have not plotted the conductance for the anisotropic s-wave gap $\Delta(\phi) = \Delta_0(0.55 + 0.45\cos 4\phi)$, since at this bias voltage it appears essentially the same as Fig. 1(b). We will show later that it can be distinguished from the $d_{x^2-y^2}$ gap at lower bias voltages, near the anisotropic s-wave gap minimum. The Fermi surface is assumed circular, although the gap is considered pinned to the lattice. Our use of a cylindrical Fermi surface is not a significant assumption since, as will be explained below, the main contribution to any signal comes from small regions of the Fermi surface.

In order to illustrate the strong angular dependence of the conductance for the $d_{x^2-y^2}$ gap, we show in Figs. 2(a) and 2(b) the conductance as a function of distance for two angles. The first angle, $\phi = 0$, is the direction of a gap maximum. The second angle, $\phi = \pi/4$, is the direction of a node. For comparison we show in Fig. 2(c) the conductance as a function of distance for an isotropic gap.

We will now analyze the pronounced spatial variation in Figs. 1 and 2. It is straightforward to reduce the integrations for the Green's functions to angular integrals. The result is essentially a line integral of an exponential along the energy contour surface $|\epsilon_{\mathbf{k}}| = \omega$. The main contribution to such an integral comes from regions of the contour surface where the curvature of the exponentiated factor is small. This occurs near gap minima and maxima when $\Delta_0 \lesssim \omega$. The integration near these regions provides most of the variation in the tunneling conductance and we find the following form [20] for the local contribution to the conductance in a $d_{x^2-y^2}$ superconductor for $\Delta_0 \lesssim V$:

$$\frac{dI(\rho,\phi_0,V)}{dV} = \frac{-\pi\delta\tilde{\epsilon}}{2\rho\cos\phi_0\alpha_+}\left(\frac{V^2}{V^2-\Delta_0^2}\right)^{\frac{1}{2}}\left[\sin(2\rho\beta_+\cos\phi_0) + \frac{\alpha_+}{\alpha_-}\sin(2\rho\beta_-\cos\phi_0)\right]\frac{\sin^2(\rho\sin\phi_0\Delta\phi)}{(\rho\sin\phi_0\Delta\phi)^2}, \tag{5}$$

where we define $\rho(\cos\phi_0, \sin\phi_0) = k_F\mathbf{r}$. For brevity, the solution for $-\pi/4 < \phi_0 < \pi/4$ is presented above. All other angles ϕ_0 can be mapped into this region. $\Delta\phi$ is a ρ-independent angle and $\alpha_\pm$ are the curvatures at the extrema for states above (+) and below (−) the Fermi surface (with the position-dependent factor $\rho\cos\phi_0$ factored out).

$$\alpha_\pm = \frac{\beta_\pm}{2} - \frac{\pm 2\Delta_0^2}{v_F k_F (V^2-\Delta_0^2)^{\frac{1}{2}}\beta_\pm}, \tag{6}$$

where $\beta_\pm = \left[1 \pm 2(V^2-\Delta^2)^{1/2}/v_F k_F\right]^{1/2} \sim 1$. The conductance in Eq. (5) has oscillations whose wavelength and amplitude depend on the bias. This bias dependence should help screen out spurious effects.

The isotropic-gap superconductor has no Fermi surface location where the curvature becomes smaller than elsewhere. Thus we find, as shown in Fig. 2, that the amplitude of the conductance variations is larger for the $d_{x^2-y^2}$ gap in the spatial direction corresponding to a gap extremum than the amplitude for the isotropic gap. The conductance for the isotropic-gap superconductor is given by the expression in Eq. (5) with the $\sin^2(\rho\sin\phi_0\Delta\phi)/(\rho\sin\phi_0\Delta\phi)^2$ and $\cos\phi_0$ factors absent and $\alpha_\pm = \beta_\pm/2$.

In Fig. 3 we show the normalized conductance for the anisotropic s-wave gap and the $d_{x^2-y^2}$ gap at a bias $V = 0.16\Delta_0$ (this is just above the minimum gap for the anisotropic s-wave gap). The isotropic gap is not shown because there is no variation in its conductance due to the impurity at this bias. Figures 3(a) and 3(b) show the change in the tunneling conductance for the anisotropic s-wave gap as a function of distance in the direction of the gap minimum and maximum, respectively. The bias is close to the minimum, so there is a long-range enhanced signal only for (a). In contrast to (a) and (b), the change in conductance for the $d_{x^2-y^2}$ gap in the same directions, shown in (c) and (d), is small.

Here we have shown that there is a characteristic struc-

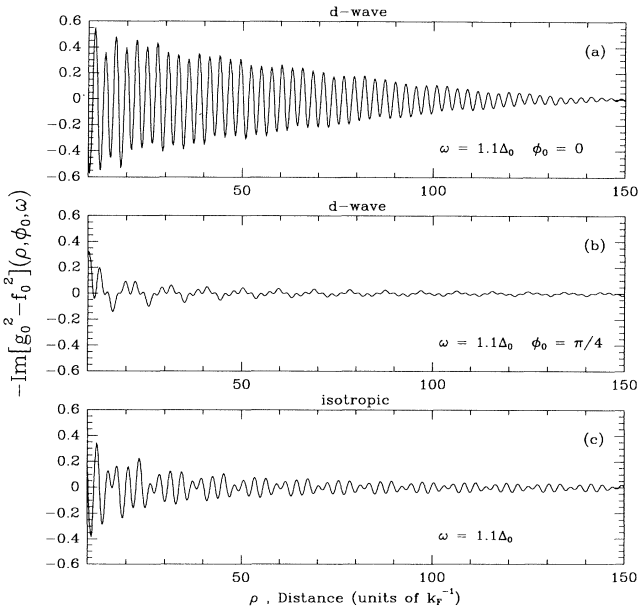

FIG. 2. Same function as Fig. 1. (a) Radial plot of the change in the conductance due to $\delta\tilde{\epsilon}$ along the high-signal direction $\phi = 0$ for the $d_{x^2-y^2}$ gap. (b) Radial plot along the low-signal direction, $\phi = \pi/4$. (c) Radial plot for the isotropic gap. The scale is the same for all three plots.

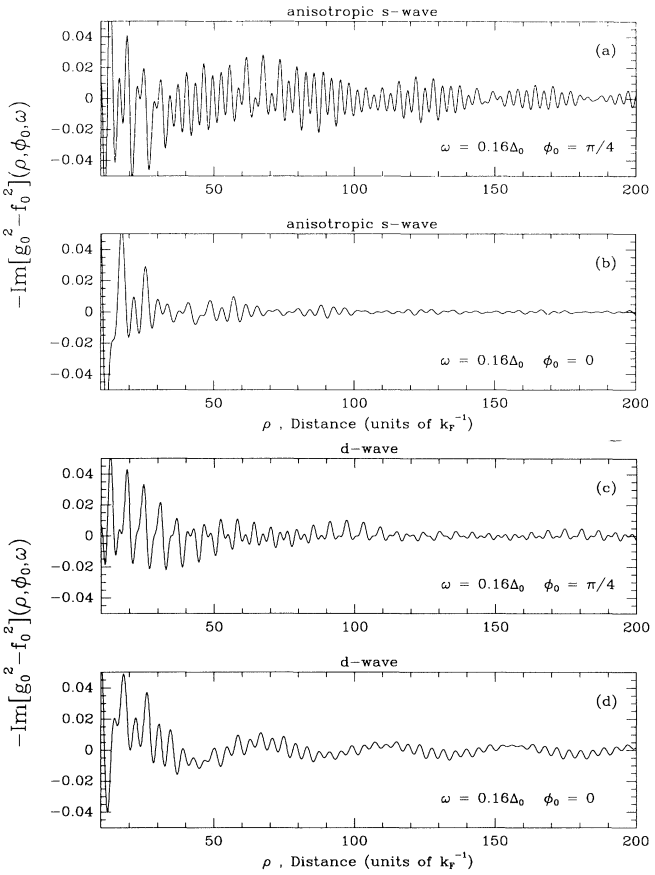

FIG. 3. Normalized conductance for a unit perturbation to the site energy $\delta\tilde{\epsilon}$. Here the voltage, $0.16\Delta_0$, is just above the gap minimum for the case of an anisotropic s-wave gap $\Delta(\phi) = \Delta_0(0.55 + 0.45\cos 4\phi)$. Radial plots of the change in conductance due to $\delta\tilde{\epsilon}$ for the anisotropic s-wave gap are shown in the direction of the gap minimum (a) and gap maximum (b). Since the bias is close to the minimum, only (a) has a long-range enhanced signal. For comparison, the same functions for the $d_{x^2-y^2}$ gap are shown in (c) and (d). Compared to (a), all three of (b), (c), and (d) are small. Thus we find a strong dependence of the tunneling conductance on gap minima, similar to the dependence on gap maxima shown in Figs. 1 and 2.

ture in the local conductance at bias voltages near gap minima or maxima which can be used to probe the momentum dependence of $\Delta_{\mathbf{k}}$. Thus one can obtain information about the symmetry of the gap. Beyond this, we believe that scanning tunneling microscopy of the local density of states around an impurity site can provide detailed information about both the momentum and frequency dependence of the gap. This would provide a means of determining both the momentum and frequency dependence of the interaction responsible for pairing in the cuprate superconductors.

J.M.B. and D.J.S. acknowledge the support of the National Science Foundation Grant No. DMR92-25027. M.E.F. acknowledges the support of this work by the National Science Foundation under Grant No. PHY89-04035.

* Present address: Division of Applied Sciences, Harvard University, Cambridge, MA 02138.

[1] G.M. Éliashberg, Zh. Eksp. Teor. Fiz. **38**, 966 (1960) [Sov. Phys. JETP **11**, 696 (1960)].
[2] K. Miyake, S. Schmitt-Rink, and C.M. Varma, Phys. Rev. B **34**, 6554 (1986); D.J. Scalapino, E. Loh, Jr., and J.E. Hirsch, Phys. Rev. B **34**, 8190 (1986).
[3] N.E. Bickers, D.J. Scalapino, and R.T. Scalettar, Int. J. Mod. Phys. B **1**, 687 (1987); N.E. Bickers, D.J. Scalapino, and S.R. White, Phys. Rev. Lett. **62**, 961 (1989); P. Monthoux, A.V. Balatsky, and D. Pines, Phys. Rev. Lett. **67**, 3448 (1991); P. Monthoux and D. Pines, Phys. Rev. Lett. **69**, 961 (1992).
[4] N. Bulut, D.J. Scalapino, and S.R. White, Phys. Rev. B **47**, 6157 (1993).
[5] W.L. McMillan and J.M. Rowell, in *Superconductivity I*, edited by R.D. Parks (Marcel Dekker, New York, 1969), p. 561.
[6] R.R. Joyce and P.L. Richards, Phys. Rev. Lett. **24**, 1007 (1970).
[7] For example, D. Mandrus *et al.*, Europhys. Lett. **22**, 199 (1993).
[8] For example, M.J. Sumner, J.-T. Kim, and T.R. Lemberger, Phys. Rev. B **47**, 12248 (1993); D. Mandrus *et al.*, Phys. Rev. Lett. **70**, 2629 (1993).
[9] S.E. Stupp, W.C. Lee, J. Giapintzakis, and D.M. Ginsberg, Phys. Rev. B **45**, 3093 (1992).
[10] W.N. Hardy *et al.*, Phys. Rev. Lett. **70**, 3999 (1993).
[11] C. Broholm *et al.*, Phys. Rev. Lett. **65**, 2062 (1990).
[12] B.O. Wells *et al.*, Phys. Rev. B **46**, 11830 (1992); Z.-X. Shen *et al.*, Phys. Rev. Lett. **70**, 1553 (1993).
[13] D.A. Wollman *et al.*, Phys. Rev. Lett. **71**, 2134 (1993).
[14] M.E. Flatté, Phys. Rev. Lett. **70**, 658 (1993).
[15] M.E. Flatté, S. Quinlan, and D.J. Scalapino, Phys. Rev. B **48**, 10626 (1993).
[16] C.H. Choi and P. Muzikar, Phys. Rev. B **41**, 1812 (1990); T.A. Tokuyasu, D.W. Hess, and J.A. Sauls, Phys. Rev. B **41**, 8891 (1990), have studied the anisotropic spatial variations in the superfluid density and current around an impurity and vortex, respectively, in an anisotropic superconductor.
[17] M.F. Crommie, C.P. Lutz, and D.M. Eigler, Nature (London) **363**, 524 (1993).
[18] A. Chang *et al.*, Phys. Rev. B **46**, 5692 (1992).
[19] For example, J.R. Schrieffer, *Theory of Superconductivity* (Benjamin/Cummings, Reading, MA, 1964).
[20] The stationary-phase approximation is sufficient to obtain the $\phi_0 = 0$ solution. Further arguments are necessary to obtain the nonzero ϕ_0 solution. The $\alpha_\pm \to 0$ divergences are cut off.

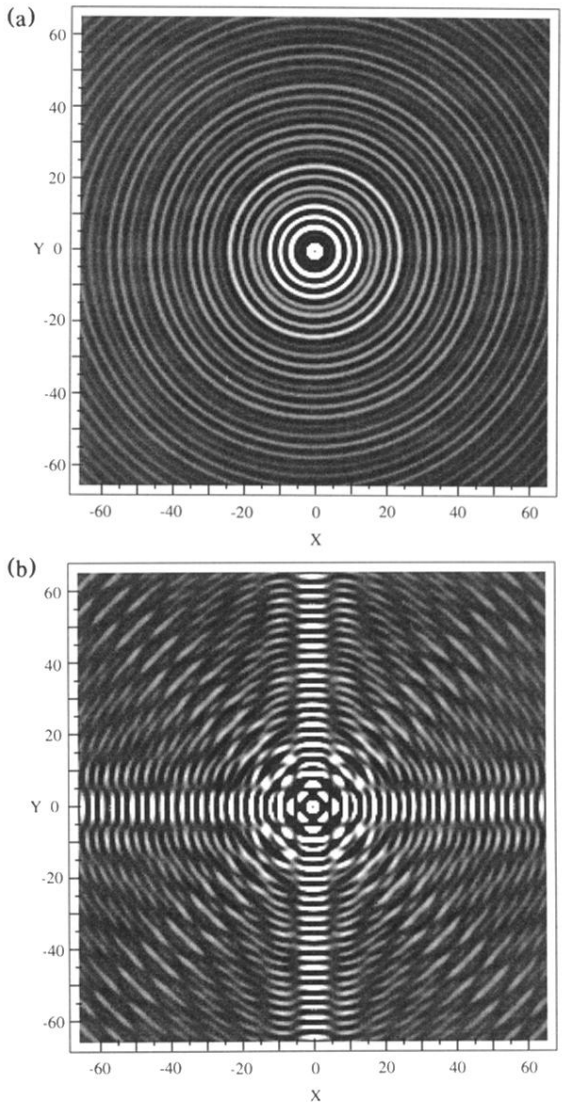

FIG. 1. Normalized conductance for a unit perturbation to the site energy $\delta\tilde{\epsilon}$. The length scale is set by k_F^{-1}. Here we have taken a coherence length equal to $10k_F^{-1}$. The voltage is $1.1\Delta_0$, where Δ_0 is the gap maximum. The range of the intensity is from -0.1 (black) to 0.1 (white). (a) Isotropic gap, $\Delta(\phi) = \Delta_0$; (b) $d_{x^2-y^2}$ gap, $\Delta(\phi) = \Delta_0 \cos 2\phi$.